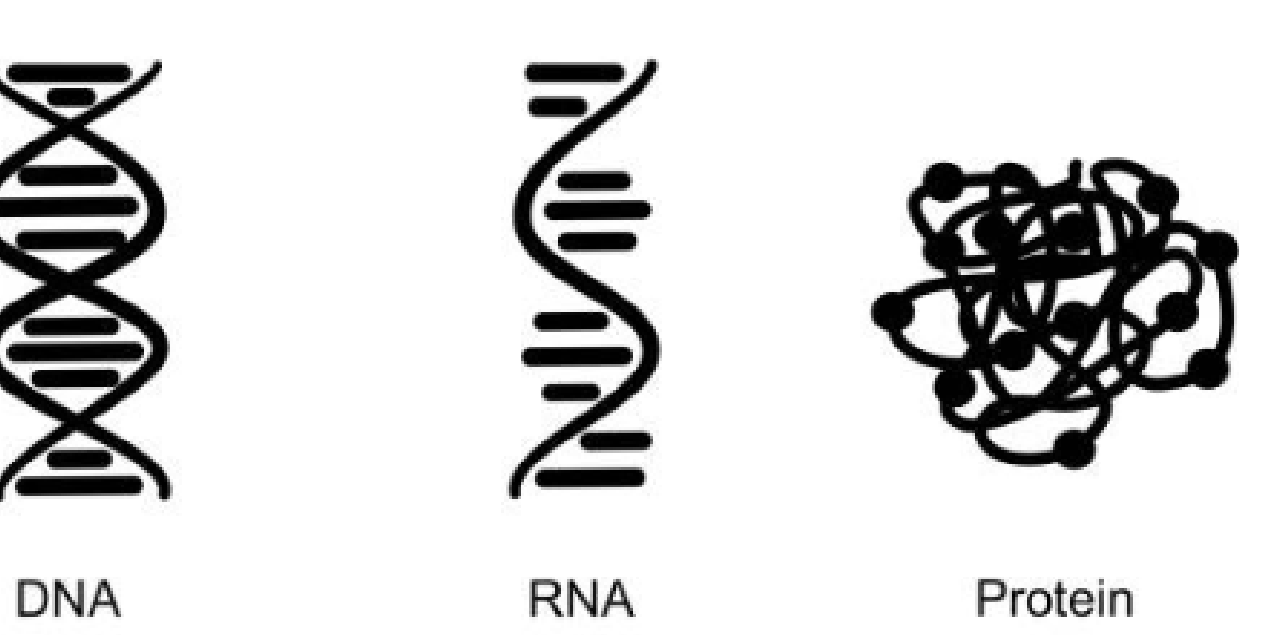


Probing RNA Base Pairing and Ligand Interactions In Solution with Infrared-based Microfluidic Modulation Spectroscopy

REDSHIFT Bio

See change®

Scott Gorman*, Valerie I. Collins, Richard Huang, Eugene Ma, David Sloan
RedShift BioAnalytics, Inc., 80 Central Street, Boxborough, MA 01719, USA
*Poster Presenter



Abstract

RNA structure and dynamics play critical roles in regulating biological processes. Understanding the conformational landscape is essential for unraveling RNA functionality, stability, and use as both a therapeutic and a therapeutic target. Microfluidic Modulation Spectroscopy (MMS) is a novel solution-state infrared spectroscopy technique that is sensitive to changes in nucleic acid base conformation and hydrogen bonding patterns. The studies detailed here utilize the latest generation of MMS instrumentation from RedShiftBio, the AuroraTX.

In these studies, we build the case for the use of MMS in RNA structural analysis. First, we present MMS IR spectra of individual RNA nucleotides, as well as polyA and polyU RNAs, showcasing the Amide I IR spectra of unpaired nucleotides. Second, we highlight the ability of MMS to resolve i-motif and G-quadruplex secondary structures in polyC and polyG RNAs, respectively. Third, we investigate GC, AU, and GU base pairing using self-complementary duplexed RNAs, demonstrating the capacity of MMS to detect and distinguish different types of base pairing. Finally, thermal melt data for GC and AU duplexes reveal the ability of MMS to monitor the melting dynamics and melting temperature of specific base-pairing interactions.

In addition to measuring native RNA structure, MMS can also detect structural changes caused by ligand binding. To demonstrate this, we present MMS data on interactions between S-adenosylmethionine (SAM) and the SAM-I riboswitch, as well as PreQ1 and the PreQ1 riboswitch. This pair of studies demonstrate the potential utility of MMS as a functional assay in the discovery of small molecule therapeutics that modulate RNA structure.

Our findings establish MMS as a powerful tool for investigating RNA structure, base-pairing dynamics, and ligand-induced conformational changes, laying the foundation for integrating the AuroraTX platform into future RNA-targeted and RNA-based therapeutic development.

Introduction

Microfluidic Modulation Spectroscopy (MMS) is an emerging infrared-based technique that provides label-free, aqueous structural analysis of biomolecules with high sensitivity. Unlike traditional infrared spectroscopy, which suffers from solvent background interference and low sensitivity, MMS employs microfluidic flow-based modulation to subtract background noise in real time, enabling precise detection of molecular structural features. By measuring IR absorption in the Amide I region, MMS captures detailed spectral changes in protein secondary structure and nucleic acid base hydrogen bonding patterns.

In this study, we demonstrate how MMS enables structural characterization of RNA, from unpaired nucleotides to structured RNA, including small self-complementary duplexes, riboswitches, i-motifs, and G-quads. Thermal ramping of these duplexes in particular demonstrates our ability to add base type granularity to thermal ramping experiments. We also demonstrate MMS's ability to detect ligand-induced conformational changes in the SAM I and PreQ1 riboswitches. Finally, we use MMS to detect the presence of G-quads as well as changes in i-motif base pairing induced by the introduction of an ionizable lipid adduct to polyC. These findings establish MMS as a powerful analytical tool for RNA research, with potential applications in RNA-targeted drug discovery and therapeutic development as well as basic research on RNA base pairing and folding.

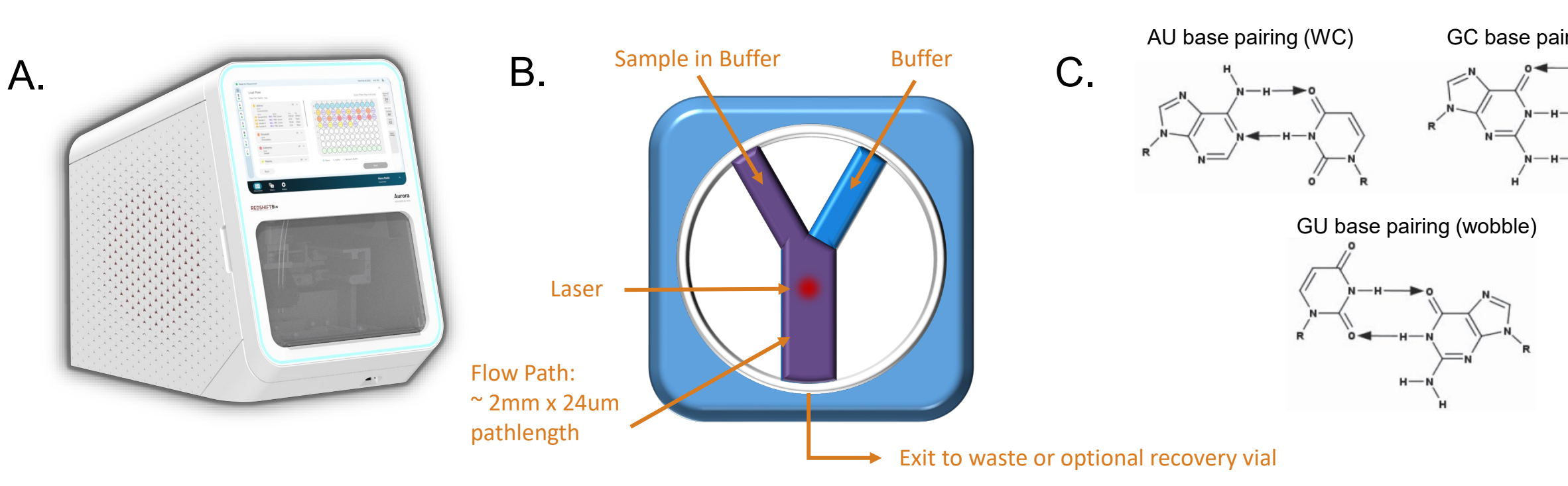
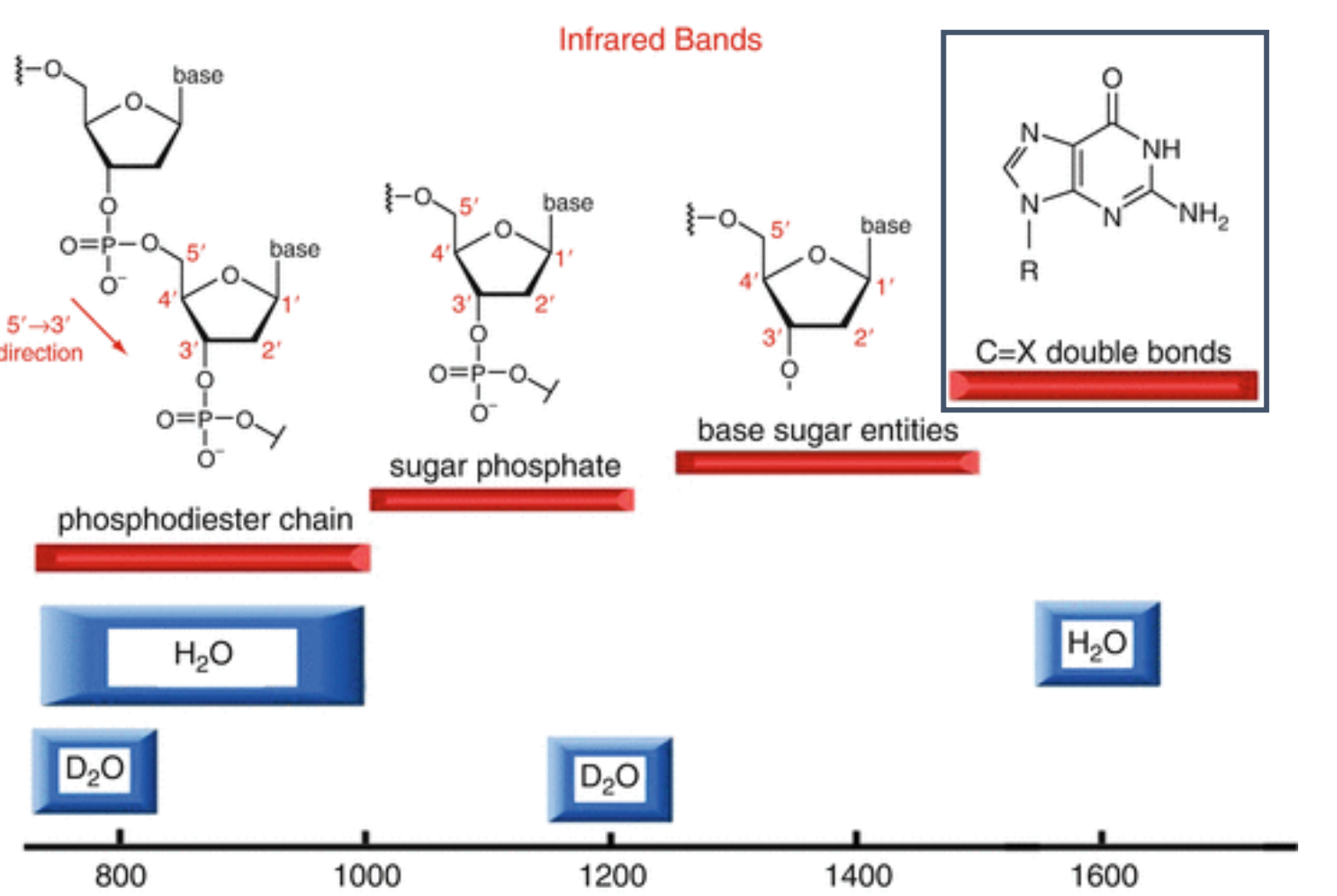


Figure 1. (A) MMS AuroraTX system (RedShiftBio) used for secondary structure analysis (B) MMS flow cell. (C) RNA base pairing¹

Background: MMS-base IR spectroscopy can measure previously hard-to-access RNA base C=O, C=C, C=N, and NH2 bands in H₂O-based solutions

IR Bands for nucleic acids:

- Nucleic acids contain functional groups that absorb in the 1750-600 cm⁻¹ infrared region.
- Water also absorbs strongly in the 1000-700 cm⁻¹ and 1550-1750 region, obfuscating nucleic acid absorbances and necessitating traditional IR experiments be performed in D₂O.
- MMS, with its near-simultaneous background measurement and subtraction, allows for studies in the 1765-1588 cm⁻¹ region in H₂O-based solutions.



Assignment	Wave number (cm ⁻¹) ^{4,5}
Base vibrations	1800-1500
Double-helical structures	1673-1660 to 1689-1678
Thermal denaturation	1696-1684, 1677-1653
Triple-helical structures	1500-1250
Base-sugar vibrations	1495-1476
Interaction involving the N7 sites of purines	1381-1369
Anti/syn conformation	1344-1328
Sugar conformations	1250-1000
Sugar-phosphate vibrations	1000-800
Backbone conformation, PO ₂ - stretching band	B-form double helix = 1225 cm ⁻¹ A-form = 1240 cm ⁻¹ Z-form = 1215 cm ⁻¹
Sugar vibrations	900-700
Sensitivity to sugar conformation	N-type sugars, 882-877, 865-860 S-type sugars, 842-820
Contribution from POP vibration	840-800

Results

Nucleosides and Polynucleotides:

- Nucleotides and nucleosides have a strong signal in the amide I band in the IR spectrum enabling the characterization by MMS.⁶
- Characterizing each nucleoside and the polynucleotides provides a foundation for more complicated structures like base pairing, G-quads, noncanonical base pairing, loops, hairpins, bulges and more.

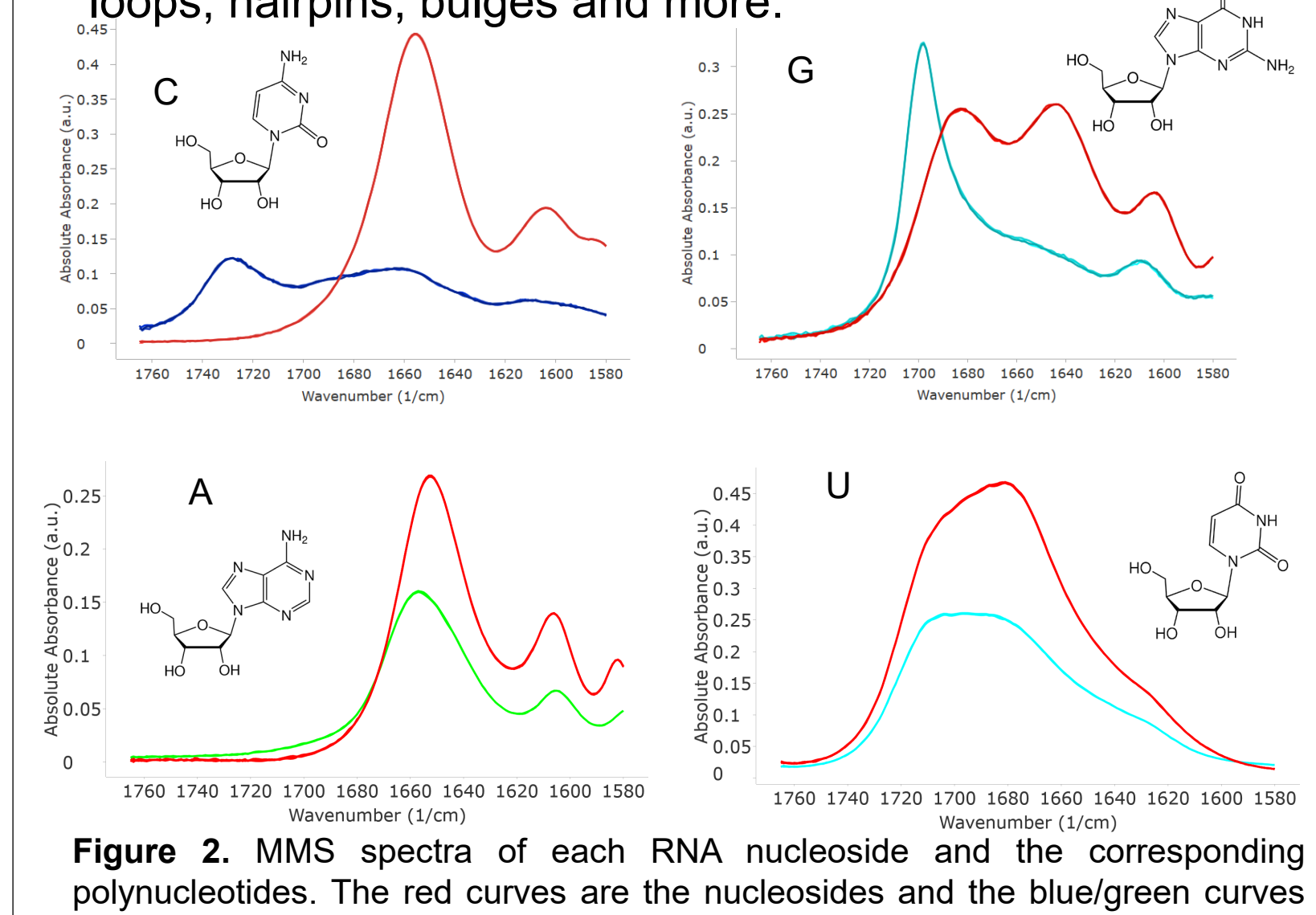


Figure 2. MMS spectra of each RNA nucleoside and the corresponding polynucleotides. The red curves are the nucleosides and the blue/green curves are the polynucleotides.

PolyC i-motif:

- PolyC and polyG both showed significantly different spectra compared to the nucleoside data in Figure 2.
- To investigate this further, we tested the pH dependence of polyC as it is known to form the i-motif in acidic conditions.⁷
- Our results show that at pH 7 and 10, the results have the same spectral features as the cytidine spectrum, indicating no extra base pairing within itself.
- In water and at pH 5, the spectra have much smaller peaks at 1660 and 1600 cm⁻¹ and an additional peak around 1730 cm⁻¹.
- The decrease in intensity is expected as the nitrogenous base is the absorbing component in MMS. Therefore, adding the backbone will add mass to the sample concentration, but not contribute to the signal, as all samples were tested at 1 mg/mL.

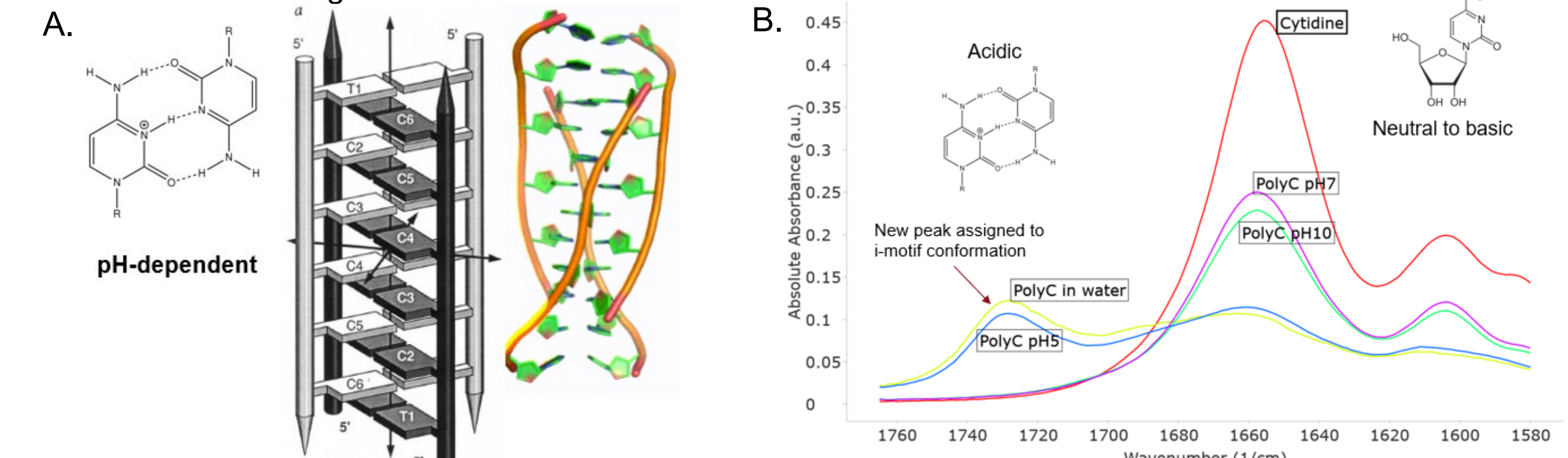


Figure 3. (A) Structure of the polyC i-motif under acidic conditions.⁵ (B) MMS spectra of polyC under various pH conditions to show the difference between unbound polyC and the proposed i-motif.

Results

Lipid Adducts:

- Therapeutic mRNA drugs are formulated in lipid nanoparticles (LNPs) to deliver the mRNA to the proper organ where it can be transcribed.
- However, it has been observed that nucleobases can be modified by the ionizable lipids and can cause a decrease in the mRNA structure and stability.
- This modification involves the ionizable lipid to covalently bond to the nucleobase, resulting in a lipid adduct to the RNA molecule it is attached to.
- In this study we used polyC at both pH 7 and pH 5 (i-motif) as the example RNA and SM-102 as the lipid.
- The adduct reaction was completed following the procedure from the Packer et al. publication.⁸ Treated samples displayed a reduction in i-motif base pairing at pH 5 compared to the control.

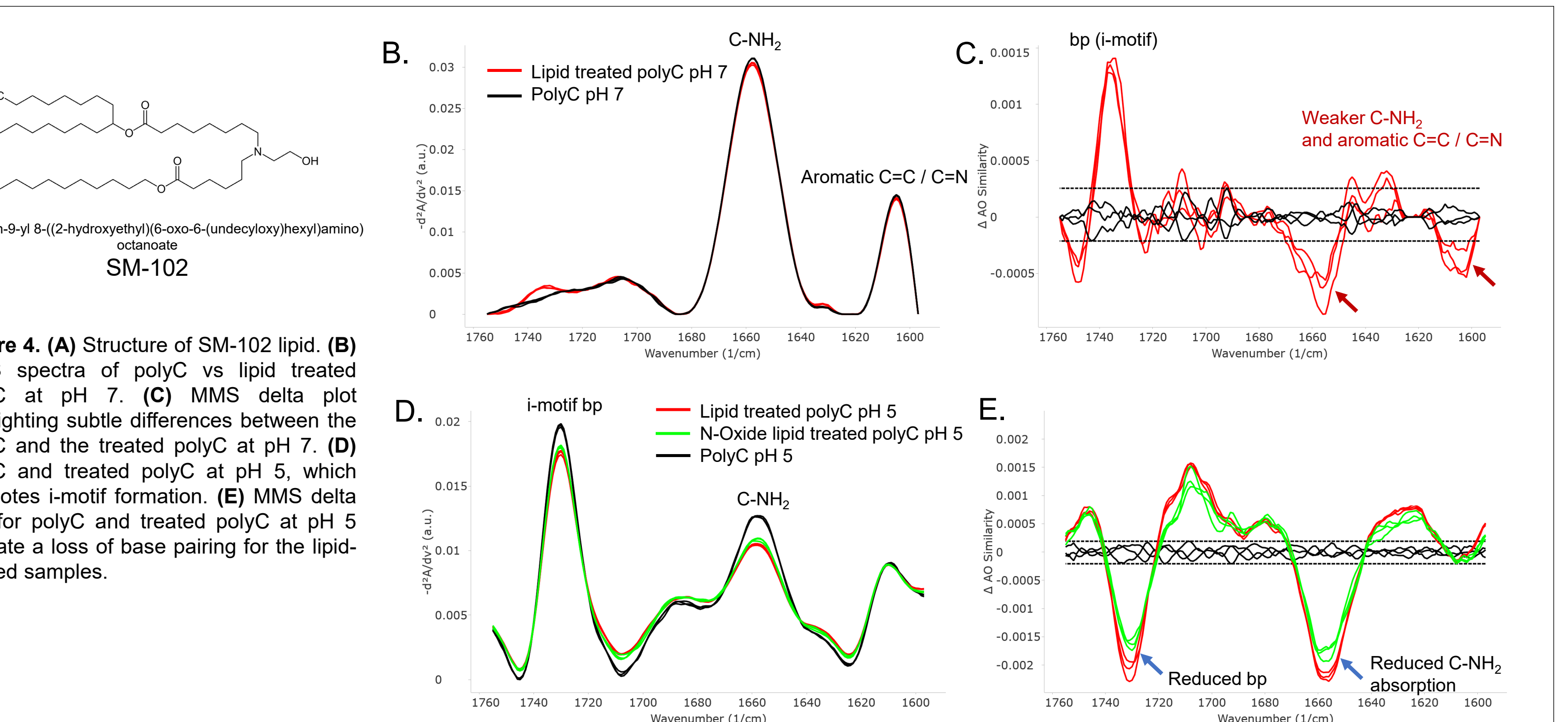


Figure 4. (A) Structure of SM-102 lipid. (B) MMS spectra of polyC vs lipid treated polyC at pH 7. (C) MMS delta plot highlighting sub differences between the lipid treated polyC at pH 7 and polyC at pH 5. (D) polyC and treated polyC at pH 5, which promotes i-motif formation. (E) MMS data plot for polyC and treated polyC at pH 5 which indicates a loss of base pairing for the lipid-treated samples.

Results

Base Pairing (GC):

- Watson-crick base pairing was characterized by designing small constructs that are energetically favorable to pair with itself and analyzed on an Aurora TX.
- Each construct underwent an annealing process to minimize the free energy and promote complete base pairing.
- Comparing the MMS spectra of the annealed construct to the mathematically averaged spectra of the components highlights the difference base pairing makes in the MMS signal.

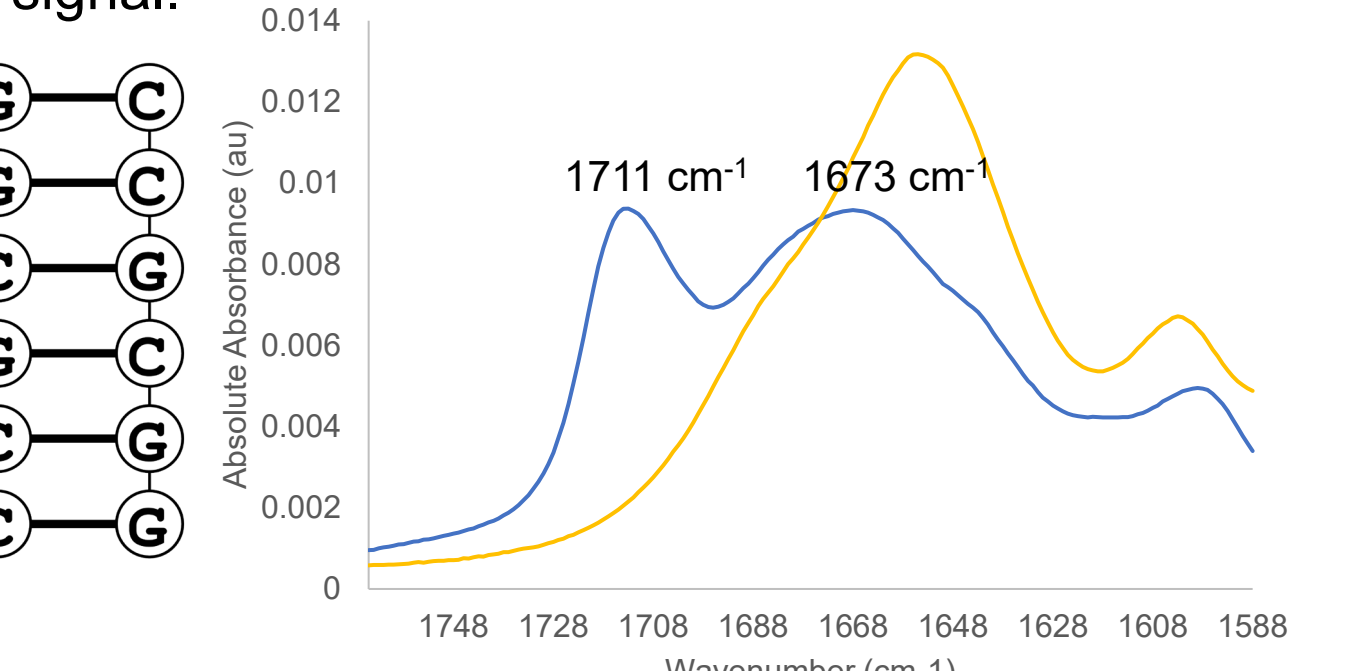


Figure 5. GC construct shown as a fully paired dimer and the MMS spectra showing the experimentally obtained base paired sample compared to the mathematically averaged spectrum from the individual nucleoside components (representing the unpaired construct).⁹

Base Pairing (AU):

- The AU construct is significantly longer than the GC construct due the fewer hydrogen bonds made between A and U, however, this construct is still predicted to fully base pair with itself.
- The AU construct (PDB ID: 1RNA¹⁰) and the crystal is shown in Figure 6.
- There are distinct spectral changes upon AU binding, specifically at 1707 and 1670 cm⁻¹.

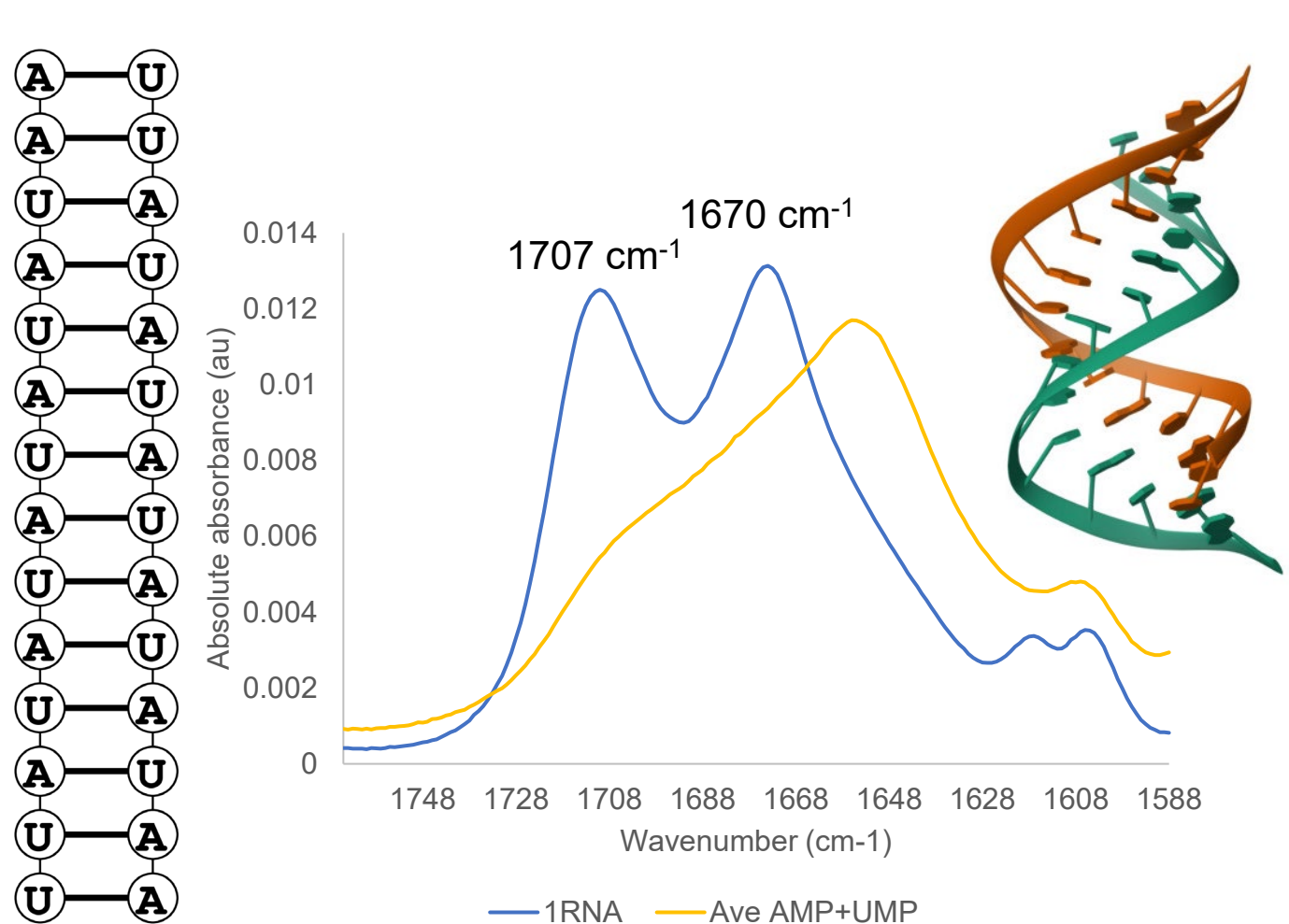


Figure 6. AU construct shown as a fully paired dimer and the MMS spectra showing the experimentally obtained base paired sample compared to the mathematically averaged spectrum from the individual nucleoside components (representing the unpaired construct).⁹

Base Pairing (GU wobble):

- GU wobble is a common noncanonical pairing that is observed in structures like loops and hairpins.
- The construct was designed as the GC construct (6 GC Watson-Crick base pairs) with 4 GU wobble pairs interspersed to ensure base pairing.
- The MMS spectra show the regions indicated with arrows are unique to the GU construct when compared to the pure GC paired spectrum and the weighted unpaired G, U, and C average.

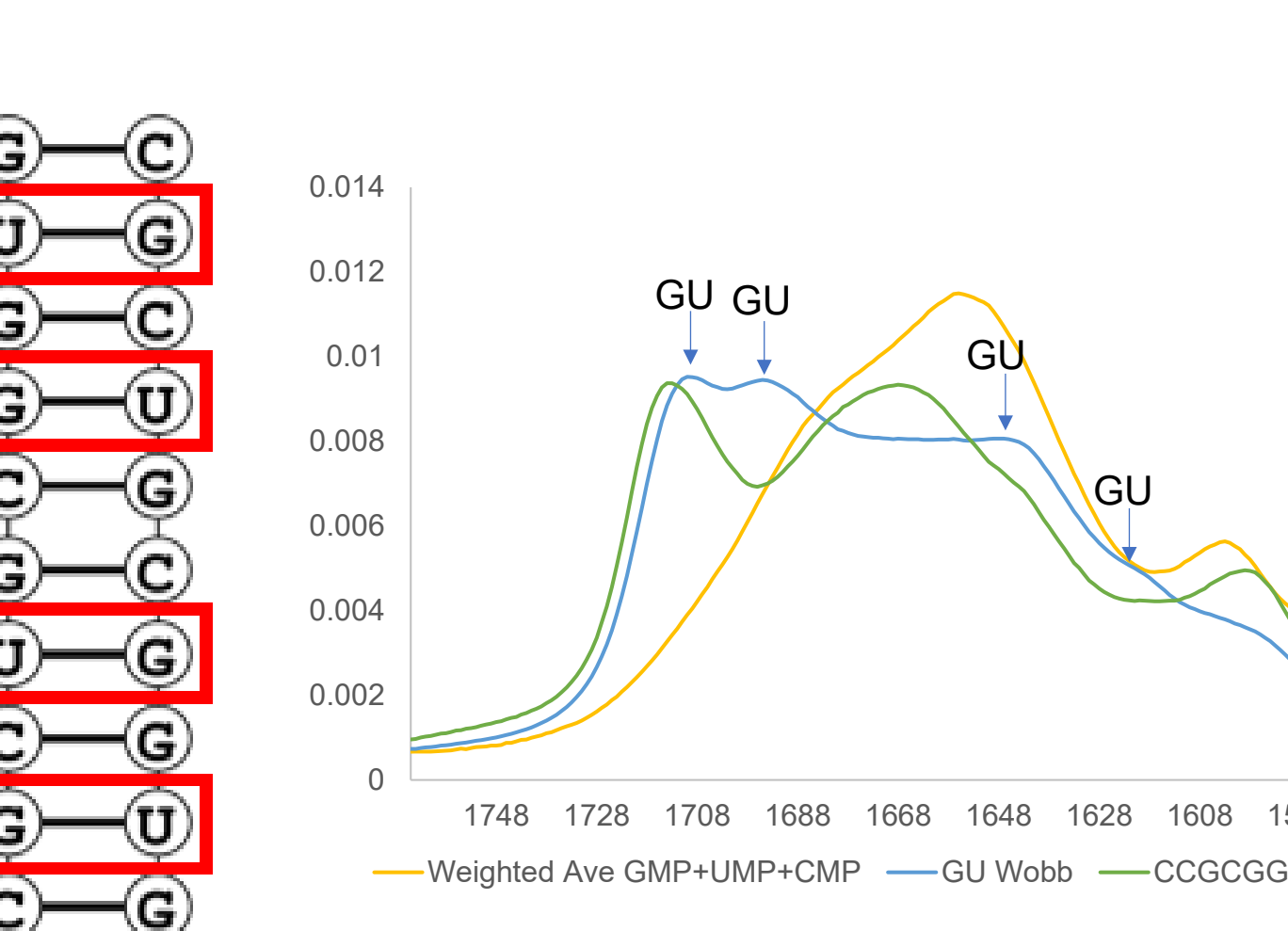


Figure 7. GU construct shown as a fully paired dimer and the MMS spectra showing the experimentally obtained base paired sample compared to the mathematically averaged spectrum from the individual nucleoside components (representing the unpaired construct).⁹

Thermal Ramping:

- Samples were thermal ramped in a stopped-flow fashion, with each modulation pulling roughly 0.5 μL of room temperature sample/buffer into a flow cell with roughly 1.5 μL of volume. Four spectra were collected at each temperature.
- Buffer used was 20 mM Sodium Phosphate, 0.5 mM EDTA, 1000 μM NaCl adjust to pH 7.0.
- As expected, the GC sample melted at a higher temperature (T_m = 67.2° C at 2 mg/mL) than the AU sample (T_m = 51.8° C at 1.75 mg/mL).

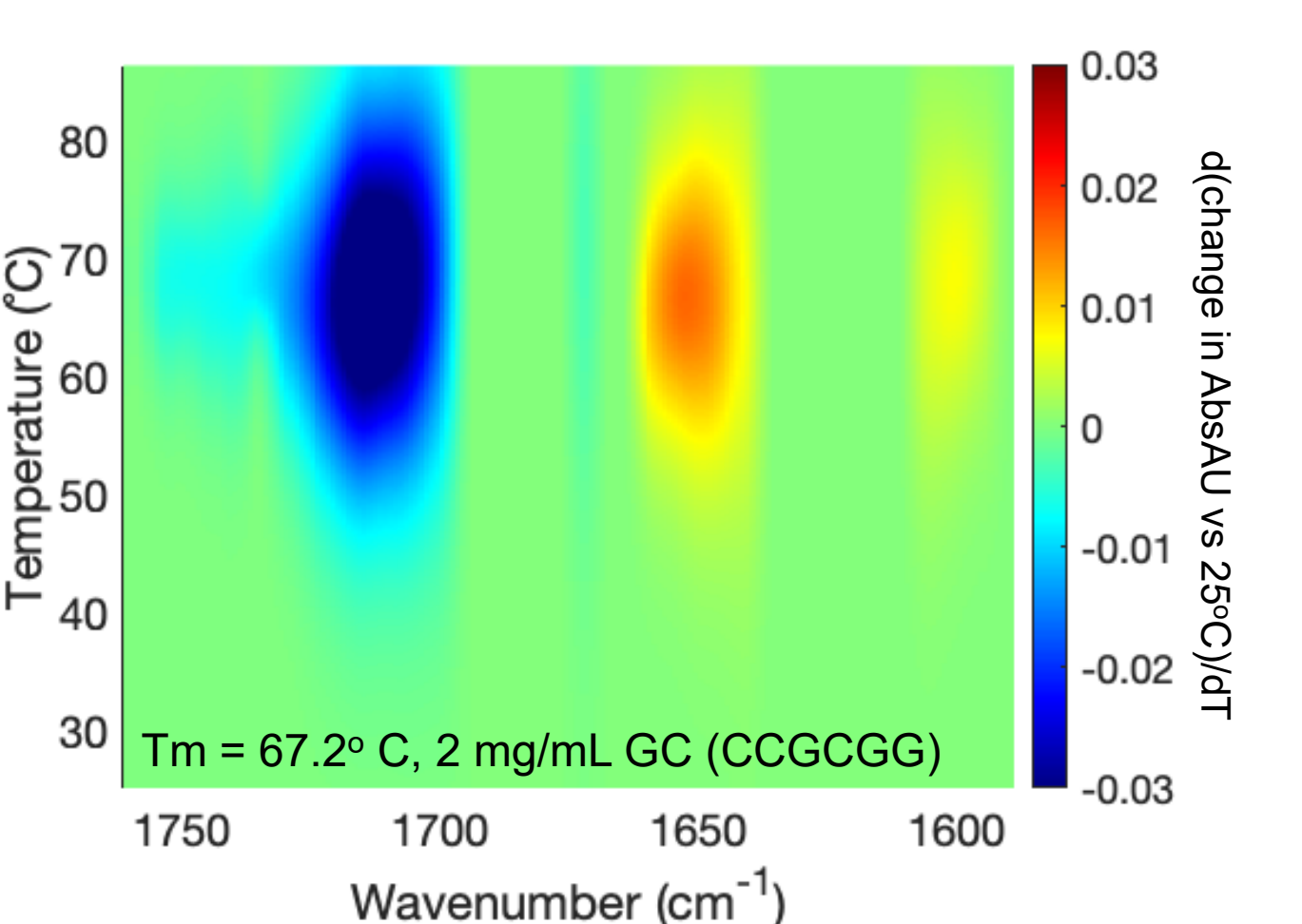


Figure 8. Thermal ramp data for the GC (CCGCGG) construct depicted as a heat map. Z-axis is the first derivative of the change in absorbance with respect to change in temperature compared to the 25° C spectrum. Blue spots indicate spectral regions where there is a loss of absorbance; red spots indicate spectral regions where there is a gain of absorbance.

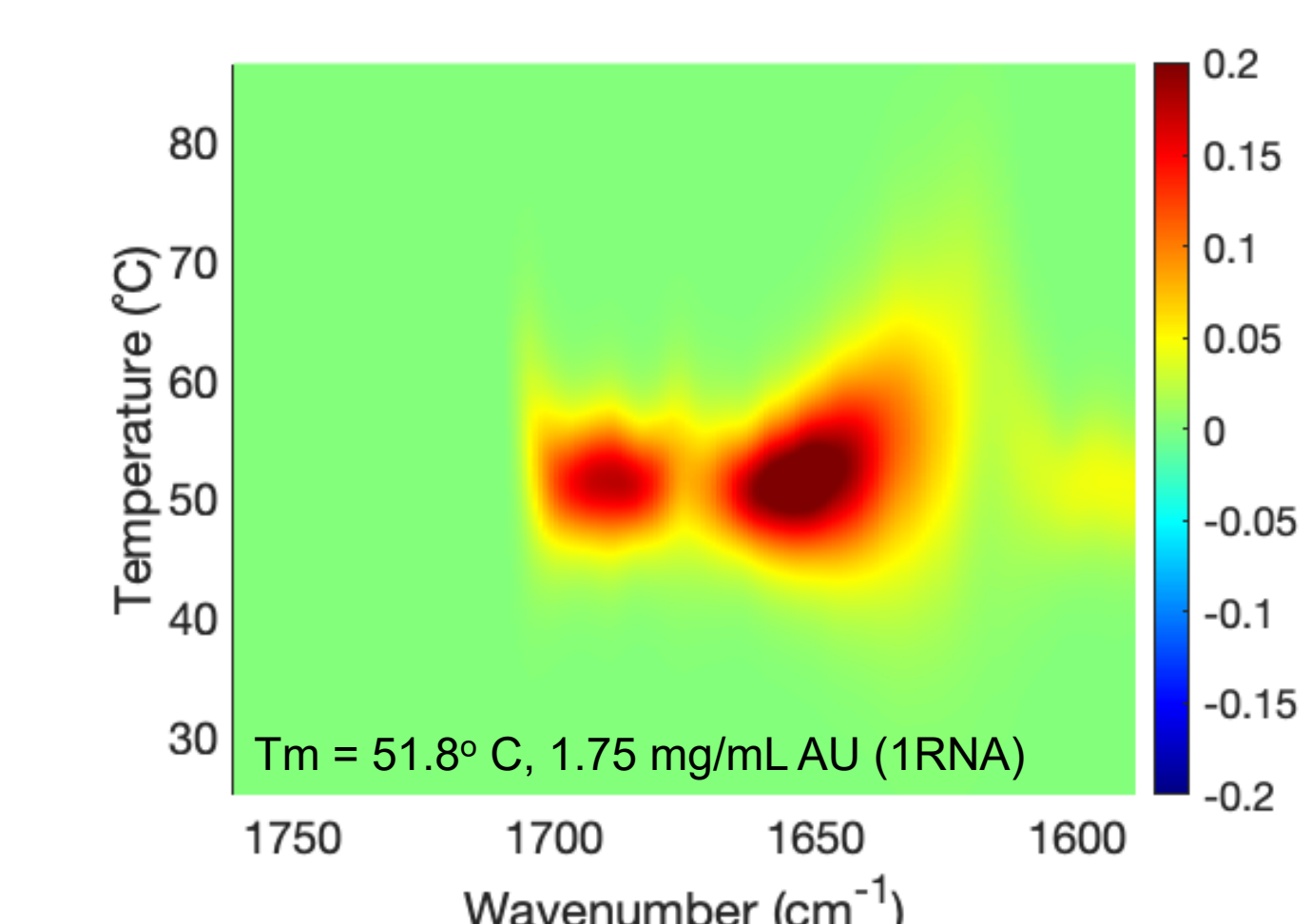


Figure 9. Thermal ramp data for the AU (1RNA) construct depicted as a heat map. Z-axis is the first derivative of the change in absorbance with respect to change in temperature compared to the 25° C spectrum. Blue spots indicate spectral regions where there is a loss of absorbance; red spots indicate spectral regions where there is a gain of absorbance.

Riboswitches (PreQ1):

- In addition to the SAM1 riboswitch, we've also studied the PreQ1 riboswitch with and without its ligand.
- The MMS spectra show distinct structure change upon ligand binding.
- Riboswitches are an important to study as models of RNA-small molecule interactions.

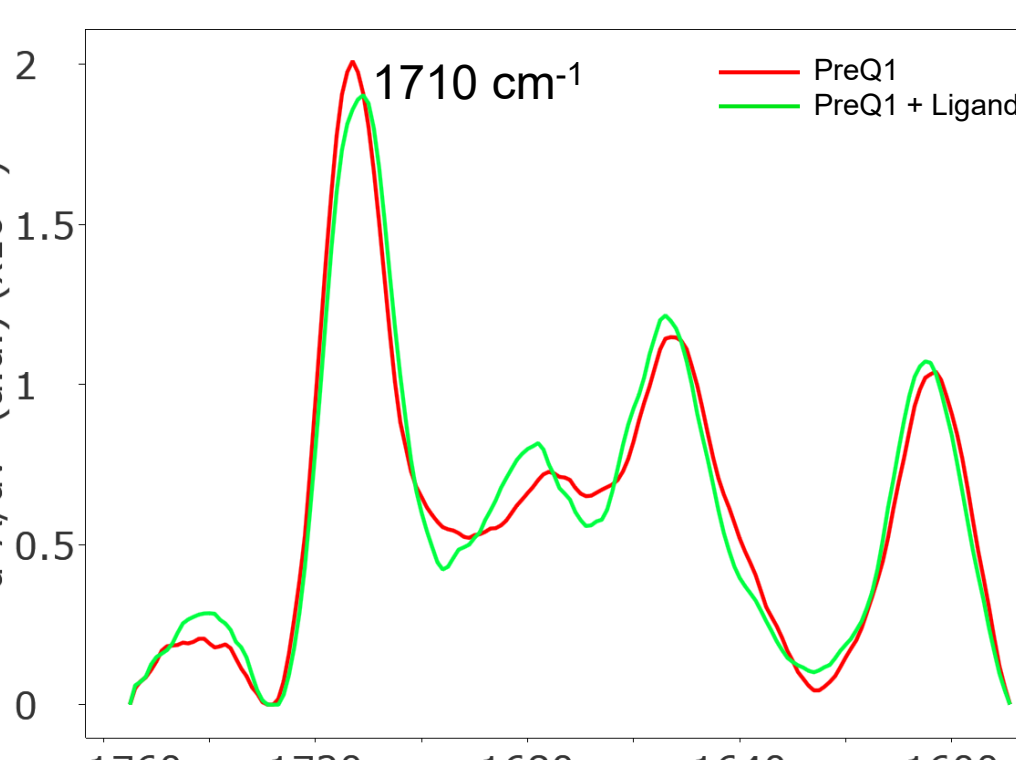


Figure 10. (A) 3D ribbon diagram of the PreQ1 riboswitch crystal structure with the small molecule ligand (SAM). (B) Schematic showing the structural change caused by ligand binding. (C) MMS spectra of SAM1 with increasing concentrations of SAM. The arrows indicate the spectral change as the SAM concentration increases from 0 to 64 μM.¹¹

Conclusions

This set of studies highlights the potential of Microfluidic Modulation Spectroscopy (MMS) in characterizing RNA base pairing and its role in RNA structure and function. MMS effectively differentiates various base-pairing interactions, including Watson-Crick, AU, and GU wobble pairs, and has the capability to monitor changes in base pairing during melts. Additionally, MMS successfully detects lipid adduct formation, demonstrating its ability to capture therapeutically relevant modifications that may impact RNA function and base-pairing dynamics. Furthermore, MMS detects ligand-induced conformational changes in riboswitches, reinforcing its potential in RNA-targeted drug discovery. These results establish MMS as an essential tool for exploring RNA base-pairing, modification, and interactions with small molecules.

Future Directions

- Further test the effect of lipid adduct formation on RNA base pairing by modifying AU, GC, and GU RNA duplexes and testing the effects of the adduct on thermal transition temperatures.
- Expand the RNA base pairing library to include more Hoogsteen and other non-canonical base pairing and test our ability to predict RNA base pairing based on spectra with chemometrics.
- Determine our LOQ for therapeutic RNA critical attributes such as dsRNA, lipid adduct formation, and polyA tail incorporation.
- Assign specific functional groups to unpaired and paired nucleobases in water (literature assignments are mostly from D₂O experiments and do not translate to H₂O-based studies well).

References

1. Agris, P. F., Eruysal, E. R., Narendran, A., et al. (2017). *RNA Biology*, 14(4), 429-440.
2. Frasson, I., Pirota, V., Richter, S. N., & Doria, F. (2022). *Methods Mol Biol* 2113:119-133.
3. Taha, F., Tran, V. D. T., & Bouchemah, A. (2017). *Methods in Molecular Biology*, 1543, 145-167.
4. Banyay, M., Sarkar, M., Graslund, A. (2003) *Biophysical Chemistry*, 104.
5. Geinguenaud, F., Militello, V., Arluisson, V. (2020). *Methods Mol Biol* 2113:119-133.
6. Huang, R., Gorman, S. (2024). *AN-850-0143*.
7. Gehring K, Leroy JL, Guérin M. (1993) *Nature*, 365:561-5.
8. Packer, M., Gyawali, D., Yerabolu, R. et al. (2021) *Nat Commun*, 12, 6777.
9. DuplexFold Web Server <https://rna.umrcc.rochester.edu/RNAstructureWeb/Servers/DuplexFold/Example.php>
10. Dock-Bregeon, A. C., et al. (1989) *J Mol Biol*, 209(3).
11. Huang, R., Collins, V., Gorman, S. (2024) *AN-850-0142*.